

Seismic Performance of Reinforced Concrete Frame Structure Based on Plastic Rotation

Kahil Amar, Meziani Faroudja, Khelil Nacim

Abstract—The principal objective of this study is the evaluation of the seismic performance of reinforced concrete frame structures, taking into account of the behavior laws, reflecting the real behavior of materials, using CASTEM2000 software. A finite element model used is based in modified Takeda model with Timoshenko elements for columns and beams. This model is validated on a Vecchio experimental reinforced concrete (RC) frame model. Then, a study focused on the behavior of a RC frame with three-level and three-story in order to visualize the positioning the plastic hinge (plastic rotation), determined from the curvature distribution along the elements. The results obtained show that the beams of the 1st and 2nd level developed a very large plastic rotations, or these rotations exceed the values corresponding to CP (Collapse prevention with $\theta_{CP} = 0.02$ rad), against those developed at the 3rd level, are between IO and LS (Immediate occupancy and life Safety with $\theta_{IO} = 0.005$ rad and $\theta_{LS} = 0.01$ respectively), so the beams of first and second levels submit a very significant damage.

Keywords—Seismic performance, performance level, pushover analysis, plastic rotation, plastic hinge.

I. INTRODUCTION

IN this study, Vecchio's experimental RC frame [16] is modeled using a CASTEM2000 finite element code by means of Timoshenko elements for columns and beams with modified model Takeda behavior [15]. The results obtained were compared with the experimental results in order to validate the finite element model [8].

After validation of the finite element model, a RC frame with 3-level and three story was modeled with the same sections as the Vecchio RC frame, in order to evaluate the level of damage of the plastic hinges (plastic rotation) in the beams, in this design, the damage to the beam results if the developed rotation exceeds the value recommended by the FAMA356 (rotation corresponding to the performance level, IOPL, LS^{PL} and CP^{PL}).

II. PRESENTATION OF THE EXPERIMENTAL MODEL

The experimental model is based upon [16], where the RC frame structure with two floors is examined and tested

Kahil Amart is with the Department of Civil Engineering, Faculty of Construction Engineering, University Mouloud Mammeri - Tizi-Ouzou B.P.17 Tizi-Ouzou 15000 (corresponding author: e-mail: amar.kahil@yahoo.com).

Meziani Faroudja is with the Department of Civil Engineering, Faculty of Construction Engineering, University Mouloud Mammeri - Tizi-Ouzou B.P.17 Tizi-Ouzou 15000 (e-mail: mfaroudja@yahoo.fr).

Khellil Nacim is with the Department of Civil Engineering, Faculty of Construction Engineering, University Mouloud Mammeri - Tizi-Ouzou B.P.17 Tizi-Ouzou 15000.

experimentally. The size and reinforcement of the structure are shown in Fig. 1. To represent constant live loads, two constant vertical forces of 700 kN each are applied over the RC Frame Structure.

A lateral displacement is imposed, and the corresponding charge is measured until the rupture of the structure.

III. MOMENT- ROTATION RELATIONS GENERATED IN THE BEAMS

The law of behavior of homogeneous sections used in this study is based on the modified Takeda model [16]. This model reflects only the bending behavior and is characterized by a trilinear moment-curvature curve (Fig. 2).

Takeda model is the model that is closest to the actual behavior of RC structures or structural elements, due to the development of cracking, microcracking and degradation of steel-concrete adhesion.

IV. PLASTIC ROTATION CALCULATION

The strain energy in the structure is dissipated by the formation of plastic hinges in the end zones of an element without affecting the rest of the structure. Several analytical models [3]-[6], [11]-[15] have developed semiempirical formulae (analytical models) in order to estimate the plastic rotation θ_p [1], [10].

The rotation of an element can be determined from the curvature distribution along the length of the element [2], [12]. Therefore, the rotation between two points, A and B (Fig. 3) is equal to the area under the curve between these two points, analytically it is given by (1):

$$\theta_{AB} = \int_A^B \phi(x) dx \quad (1)$$

where θ is the rotation of an element, x is the distance of the elementary element dx from B, and ϕ is the curvature between points A and B.

The correlation suggested by FEMA is adopted in this study to define major performance levels corresponding to the given likelihood of ground motion. FEMA-273 [7] and ATC-40 [1] described the performance levels (PL's) summarized in Table I as:

- **Immediate occupancy (IO^{PL}):** damage is relatively limited. The structure retains a significant portion of its original stiffness and strength.
- **Life safety (LS^{PL}):** substantial damage has occurred to the structure. It may have lost a significant amount of its stiffness but a substantial margin remains for additional

lateral deformation before collapse occurrence.

- **Collapse prevention (CP^{PL}):** extreme damage has

occurred. If laterally deformed beyond this point, the structure can experience instability and collapse (C^{PL}).

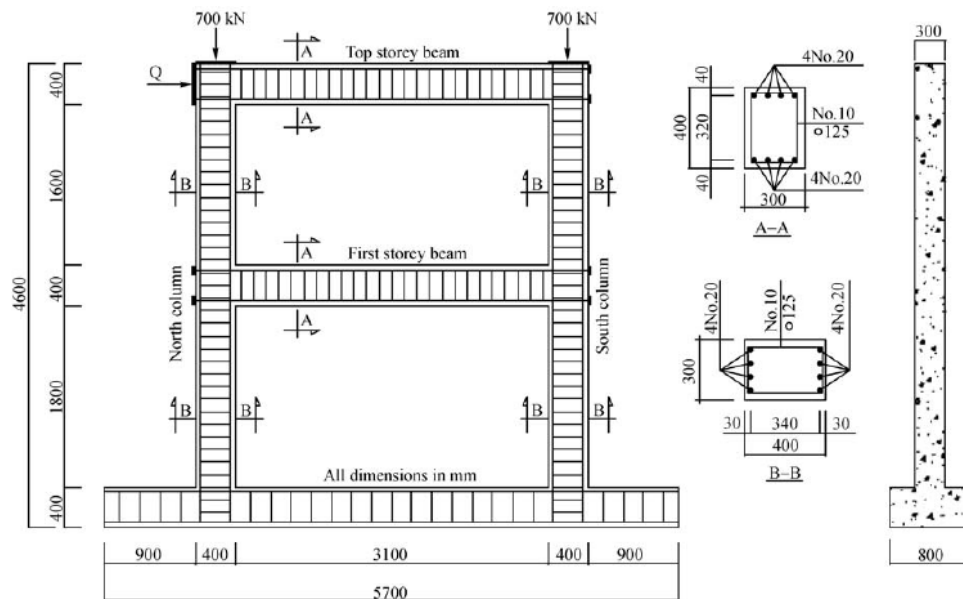


Fig. 1 Geometry and reinforcement of the experimental RC frame

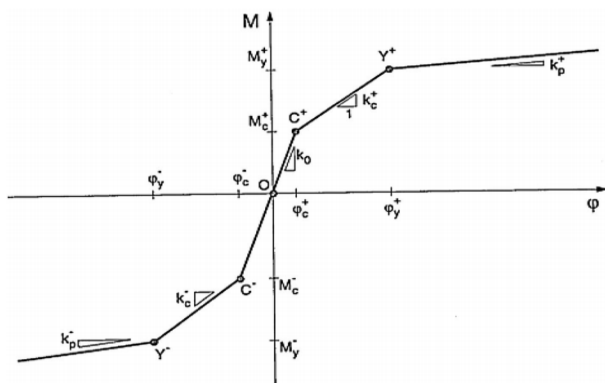


Fig. 2 Moment-curvature response of modified TAKEDA model [16]

TABLE I ACCEPTANCE CRITERIA FOR RC BEAMS GIVEN BY FEMA 273			
	Immediate occupancy (IO ^{PL})	Life Safety (LS ^{PL})	Collapse Prevention (CP ^{PL})
Plastic Rotation Angle (rad)	0.005	0.01	0.02
Description	Insignificant	Moderate	Heavy Complete

V. DESCRIPTION OF THE 3RD STOREYS CASE STUDY RC FRAME

The RC frame structure studied (Fig. 4) is composed of columns and beams of the same dimensions as the experimental RC framework, in which it added a level and two frames (The frame is having a storey height of 3.06 m and bay width of 3.5 m), see Fig. 4.

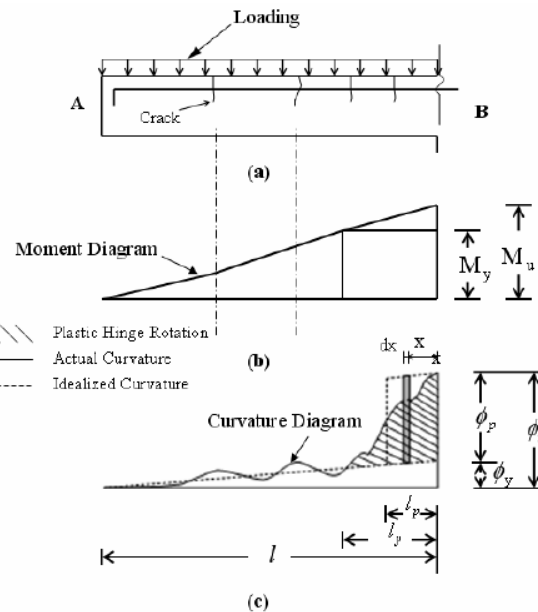


Fig. 3 (a) Beam (b) Bending Moment Diagram (c) Curvature Diagram Schematic Curvature Distribution along Beam at Ultimate Stage

To see the positioning and evolution of the rotations in the beams, Failover analysis was used [15]. The RC frame was subjected to a triangular lateral load with increasing intensity (pushed progressively) [1], [7], [9].

The lateral increasing load, at which the different structural components reach failure, is recorded according to the displacement of the roof (load displacement). This incremental

process continues until the ultimate displacement of the structure is reached (occurrence of plastic hinges).

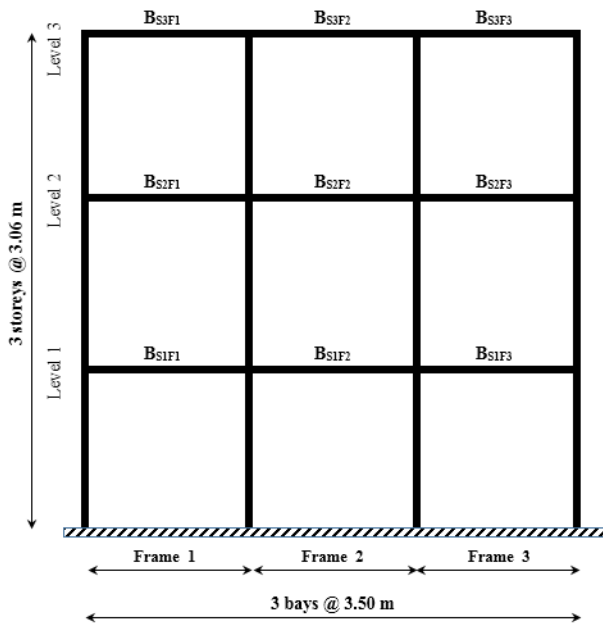


Fig. 4 The 3rd stores case study RC frame and identification of the beams

VI. MOMENT- ROTATION RELATIONS GENERATED IN THE BEAMS

Figs. 5-7 show the moment-rotation laws obtained for different beams of the RC frame, and the location of the rotation corresponding to the performance levels IO^{PL} , LS^{PL} and CP^{PL} .

We have shown in the first part the evolution of the moment as a function of the rotation in the different beams of the RC frame, which allowed us, after positioning the rotations corresponding to the IO^{PL} , LS^{PL} and CP^{PL} states, to predict the level of performance (performance level) in each beams (nodal area),

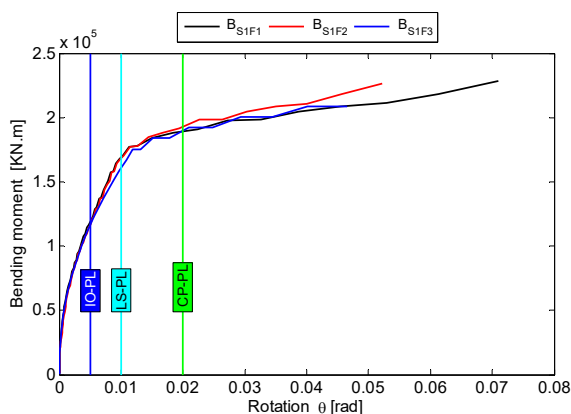


Fig. 5 Moment-rotation relations developed in the beams of RC frame (Beams of the 1st level)

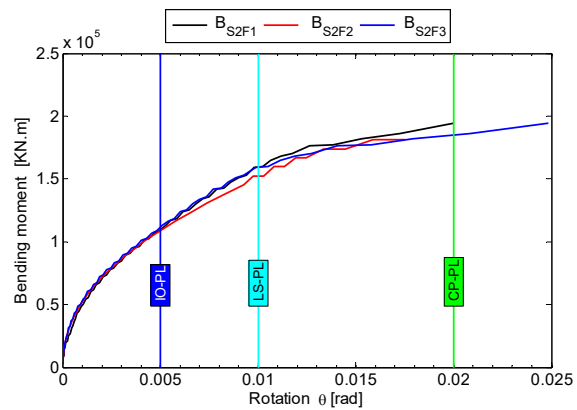


Fig. 6 Moment- rotation relations developed in the beams of RC frame (Beams of 2nd level)

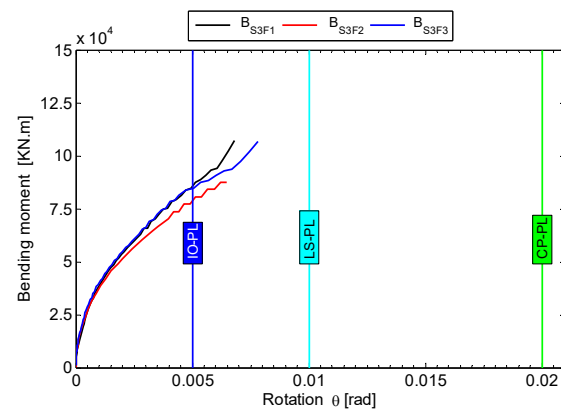


Fig. 7 Moment-rotation relations developed in the beams of RC frame (Beams of 3rd level)

The final (maximum) rotations developed in the beams of the first level of the RC frame exceed the rotations corresponding to CP^{PL} ($\theta_{CP} = 0.02$ rad), their corresponding values are of the order of 0.0522, 0.0465 and 0.0710 rad for the beams B_{S1F1} , B_{S1F2} , and B_{S1F3} , respectively.

For the beams of the second level of the RC frame, the extreme (maximum) rotations developed exceed the rotations corresponding to the CP^{PL} performance level (ie $\theta_{CP} = 0.02$ rad) for the B_{S2F3} beam to reach a value of 0.0249 rad, whereas the B_{S2F1} beam has just reached the corresponding limit at the LS^{PL} performance level (with $\theta_{LS} = 0.01$ rad), and for the B_{S2F2} beam, the developed rotation greatly exceeds $\theta_{LS} = 0.01$ rad to take a value of about 0.0175 rad which anticipate the limit CP^{PL} . On the other hand, the beams of the last level of the RC frame, the developed rotations, exceeding the threshold of IO^{PL} ($\theta_{IO} = 0.005$ rad), without reaching the limit ($\theta_{LS} = 0.01$ rad).

We conclude that as shown in Fig. 8, the 1st and 2nd level beams have lower performance levels (CP^{PL}). The beams of the last level exhibit a better behavior and they present important level of performance, i.e. an IO^{PL} level.

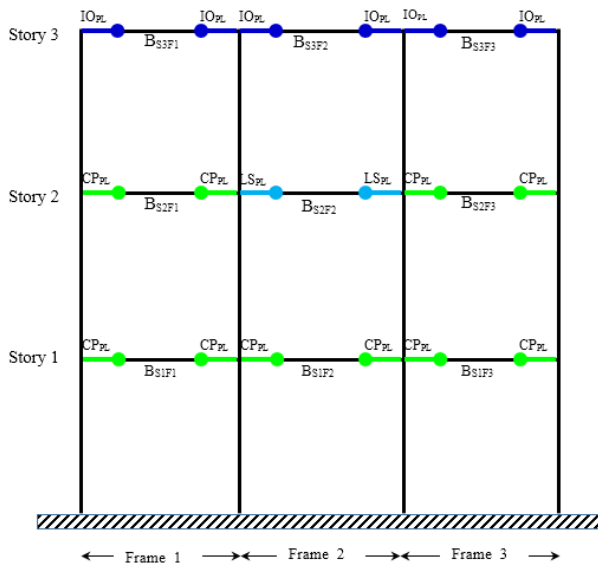


Fig. 8 Location of plastic hinges in the RC frame

VII. CONCLUSION

In this study, we have attempted to present the evolution of plastic rotation at nodes of the RC frame, while relying on the moment-rotation laws developed, and on the positioning of the limits recommended by FEMA 273, according to the results thus found, it turns out that some beams like that of the last level (Fig. 8) exceed the IO^{PL} and LS^{PL} states but without reaching the state of performance LS^{PL} and CP^{PL} , respectively. This led us to propose another methodology based on the fragility curves, where the state of damage corresponding to IO^{PL} , LS^{PL} and CP^{PL} is reached if the probability of failure reaches the value of 1.00 is IO^{CF} , LS^{CF} and CP^{CF} , (rotation corresponding to the performance level obtained by a fragility curver, IO^{CF} , LS^{CF} and CP^{CF}).

REFERENCES

- [1] ATC. Seismic evaluation and retrofit of concrete buildings. ATC 40, Redwood City: Applied Technology Council, 1996 39. Kheyroddin A, Mortezaei A. The effect of element size and plastic hinge characteristics on nonlinear analysis of RC frames. Iranian Journal of Science and Technology. Transaction B. Engineering, 2008, 2(B5): 451–470
- [2] Bae S, Bayrak O. Plastic hinge length of reinforced concrete columns. ACI Structural Journal, 2008, 105(3): 290–300 28. Chopra A K, Goel R K. A modal pushover analysis procedure for estimating seismic demands for buildings. Earthquake Engineering & Structural Dynamics, 2002, 31(3): 561–582
- [3] Baker A L L, Amarakone A M N. Inelastic hyperstatic frame analysis. ACI Structural Journal, 1964, SP-12: 85–142 42. Baker A L L. Ultimate Load Theory Applied to the Design of Reinforced and Prestressed Concrete Frames. London: Concrete Publications Ltd., 1956, p91
- [4] Bayrak O, Sheikh S A. Confinement reinforcement design considerations for ductile HSC columns. Journal of the Structural Division, 1998, 124(9): 999–1010
- [5] Berry M P, Lehman D E, Lowes L N. Lumped-plasticity models for performance simulation of bridge columns. ACI Structural Journal, 2008, 105(3): 270–279
- [6] Corley W G. Rotational capacity of reinforced concrete beams. Journal of the Structural Division, 1966, 92(ST5): 121–146 46. Herbert A, Sawyer J R. Design of concrete frames for two failure stages. ACI Structural Journal, 1964, SP-12: 405–437
- [7] FEMA. NEHRP Commentary on the Guidelines for Seismic Rehabilitation of Buildings, FEMA 273 Report, prepared by the Building Seismic Safety Council and the Applied Technology Council for the Federal Emergency Management Agency, Washington, D.C., 1997
- [8] Kahil A., Nekmouche A., Boukais S. et al. (2017), Effect of RC wall on the development of plastic rotation in the beams of RC frame structures, Frontiers of Structural and Civil Engineering, Vol. 12, No 3, pp. 318–330.
- [9] Kim S, D'Amore E. Pushover analysis procedure in earthquake engineering. Earthquake Spectra, 1999, 15(3): 417–434 32. ATC. Seismic evaluation and retrofit of concrete buildings. ATC 40, Redwood City: Applied Technology Council, 1996
- [10] Mattock A H. Rotational capacity of hinging regions in reinforced concrete beams. ACI Structural Journal, 1964, SP-12: 143–181 48. Mattock A H. Rotational capacity of hinging regions in reinforced concrete beams. Journal of the Structural Division, 1967, 93(ST2): 519–522
- [11] Mortezaei A, Ronagh H R. Plastic hinge length of FRP strengthened reinforced concrete columns subjected to both far-fault and nearfault ground motions. Scientia Iranica, 2012, 19(6): 1365–1378
- [12] Park R, Priestley M J N, Gill W D. Ductility of square-confined concrete columns. Journal of the Structural Division, 1982, 108 (ST4): 929–950
- [13] Paulay T, Priestley M J N. Seismic Design of Reinforced Concrete and Masonry Buildings. New York: John Wiley & Sons, 1992 51. Riva P, Cohn M Z. Engineering approach to nonlinear analysis of concrete structures. Journal of the Structural Division, 1990, 116(8): 2162–2186
- [14] Sheikh S A, Khoury S S. Confined concrete columns with stubs. ACI Structural Journal, 1993, 90(4): 414–431 53. Sheikh S A, Shah D V, Khoury S S. Confinement of high-strength concrete columns. ACI Structural Journal, 1994, 91(1): 100–111
- [15] Takeda, T., Sozen, M.A. and Nielsen, N.N. (1970), Reinforced Concrete Response to Simulated Earthquakes, Journal of the Structural Division, ASCE, Vol. 96, ST 12
- [16] Vecchio, F.J., and Emara, M.B. (1992), Shear Deformations in Reinforced Concrete Frames, ACI Structural Journal, Vol. 89, No 1, pp. 46–56.